MATERIALS CHEMISTRY FRONTIERS

CHINESE CHEMICAL SOCIETY | ICCAS | ROYAL SOCIETY OF CHEMISTRY

RESEARCH ARTICLE

View Article Online
View Journal | View Issue

Check for updates

Cite this: *Mater. Chem. Front.*, 2021, **5**, 4565

An encapsulation–reduction–catalysis confined all-in-one microcapsule for lithium–sulfur batteries displaying a high capacity and stable temperature tolerance†

Mengfei Zhu,‡[a] Chaoyu Yang,‡[b] Tianli Han,[a] Chaoquan Hu, *[cd] Yong Wu,[a] Ting Si *[b] and Jinyun Liu *[a]

Received 13th February 2021,
Accepted 23rd April 2021

DOI: 10.1039/d1qm00250c

rsc.li/frontiers-materials

Developing emerging host materials for constructing high energy-density lithium–sulfur (Li–S) batteries has received extensive attention. Herein, we develop a carbon nanotube (CNT)/S-infilled all-in-one microcapsule for Li–S batteries by catalytically growing CNTs using reduced Co_3O_4 nanoboxes inside a microcapsule. The encapsulation of Co_3O_4 nanoboxes into the microcapsule is achieved by using an oil-in-water emulsion. In the all-in-one microcapsule, the CNTs improve the conductivity, the microcapsule shell reduces the loss of polysulfides during cycling, and the void inside the microcapsule efficiently accommodates the volumetric change of sulfur. A Li–S battery based on the all-in-one microcapsule exhibits a high capacity of 1010 mA h g^{-1} after 250 cycles and a coulombic efficiency of $\approx$99.8%. Moreover, the battery displays stable performance when cycling at temperatures of −5 °C and 45 °C, which indicates its good potential for practical applications.

Introduction

As a widely-used energy-storage system, lithium-ion batteries have played a significant role in industrial production and daily life. However, current lithium-ion batteries have not achieved the ideal practical capacity and energy density yet. Recently, the development of emerging battery systems has been particularly important.[1] Because of the high theoretical specific capacity (1675 mA h g^{-1}) and energy density (2600 W h kg^{-1}), lithium–sulfur (Li–S) batteries have been considered promising next-generation secondary batteries.[2] However, due to the poor conductivity of sulfur, the electrochemical utilization is insufficient; the shuttle effect of polysulfides during charging and discharging results in serious capacity loss and a large volume-change.[3,4]

Engineering specific materials as potential sulfur hosts to improve the cycling stability has become a research hotspot.[5] Cui's group reported a three-dimensional (3D) electrode structure to achieve both physical encapsulation of sulfur and polysulfide binding simultaneously.[6] The prepared cathode based on TiO_2 inverse opal was conductive and robust toward electrochemical cycling; and the 3D porous structure improved the sulfur and polysulfide confinement. In addition, Ben's team prepared a carbonized nitrogen-containing porous organic framework as the sulfur host exhibiting good lithium-storage performance.[7] The micropores confined the sulfur molecules S_{2-4}; and the nitrogen-containing porous host promoted chemical adsorption of sulfur. Wang's group developed a sulfur cathode by using triple-shelled TiO_{2-x} hollow multi-shelled sphere as the host, which delivered high electrochemical performance due to a better spatial confinement and integrated conductivity of the intact triple-shell that combined the features of physicochemical adsorption, short charge transfer path and mechanical strength.[8] As seen, hollow micro/-nanostructures have displayed a good potential as the sulfur host.[9]

Recently, a polypyrrole layer coated sulfur/graphene aerogel composite has also been reported, effectively suppressing the dissolution of polysulfides through strong chemical interaction.[10] The battery exhibited discharge capacities of 1167 and 409 mA h g^{-1} at 0.2 and 5C, respectively. After 500 cycles, the capacity was 698 mA h g^{-1} at 0.5C. Sun *et al.* prepared a series of carbon-based sulfur hosts such as Fe_2N@C yolk–shell nanoboxes,[11]

[a] *Anhui Provincial Engineering Laboratory for New-Energy Vehicle Battery Energy-Storage Materials, College of Chemistry and Materials Science, Anhui Normal University, Wuhu, Anhui 241002, P. R. China. E-mail: jyliu@iim.ac.cn*
[b] *Department of Modern Mechanics, University of Science and Technology of China, Hefei, Anhui 230026, P. R. China. E-mail: tsi@ustc.edu.cn*
[c] *Nanjing IPE Institute of Green Manufacturing Industry, Nanjing 211100, Jiangsu, P. R. China*
[d] *State Key Laboratory of Multiphase Complex Systems, Institute of Process Engineering, Chinese Academy of Sciences, Beijing 100190, P. R. China. E-mail: cqhu@ipe.ac.cn*

† Electronic supplementary information (ESI) available: Experimental process, supplementary figures. See DOI: 10.1039/d1qm00250c

‡ These authors contribute equally to this work.

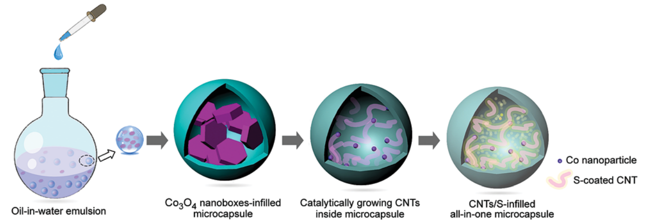

Fig. 1 Illustration of the preparation of the CNTs/S-infilled microcapsules.

Co_9S_8 decorated carbon nanoboxes,[12] and porous carbon nanoparticles interconnected with carbon nanotubes,[13] which exhibited good electrochemical performance and a long cycling life. Zhou *et al.* reported a double-shell Co_3O_4/C particle as the sulfur host.[14] The double-shell structure significantly improved the adsorption of soluble polysulfide. The prepared S@Co_3O_4/C cathode had a considerable capacity enhancement. After 500 cycles at 1C, the cathode exhibited a capacity decay of 0.083% per cycle. Liao's team reported a $Ni_xCo_{3-x}S_4$ nanocrystal-decorated nitrogen-doped carbon nanosheet.[15] The large porosity, stable carbon frame and uniform $Ni_xCo_{3-x}S_4$ nanocrystals served as strong traps for immobilizing Li_2S_n, effectively suppressing the shuttle effect and promoting the effective use of sulfur.

Herein, we develop an all-in-one microcapsule composed of carbon nanotubes (CNTs) growing inside the microcapsule as a novel sulfur host. The experimental details are displayed in the ESI.† As illustrated in Fig. 1, at first, Co_3O_4 nanoboxes were synthesized using a hydrothermal method[16] with some modifications, then they were encapsulated in a microcapsule by using an emulsion system. During the thermal treatment, Co_3O_4 was reduced to metal Co, catalysing the *in situ* growth of CNTs inside the microcapsule. Because we found that the common Co particles would aggregate severely during the microcapsule preparation and thermal reduction, which made the carbon nanotubes grow nonuniformly in the microcapsules, we used nanoboxes to improve the uniform distribution of the Co particles for catalytically growing carbon nanotubes. The prepared microcapsule was further used as the sulfur host for constructing a Li–S battery, which exhibited high electrochemical performance including good capacity and stability.

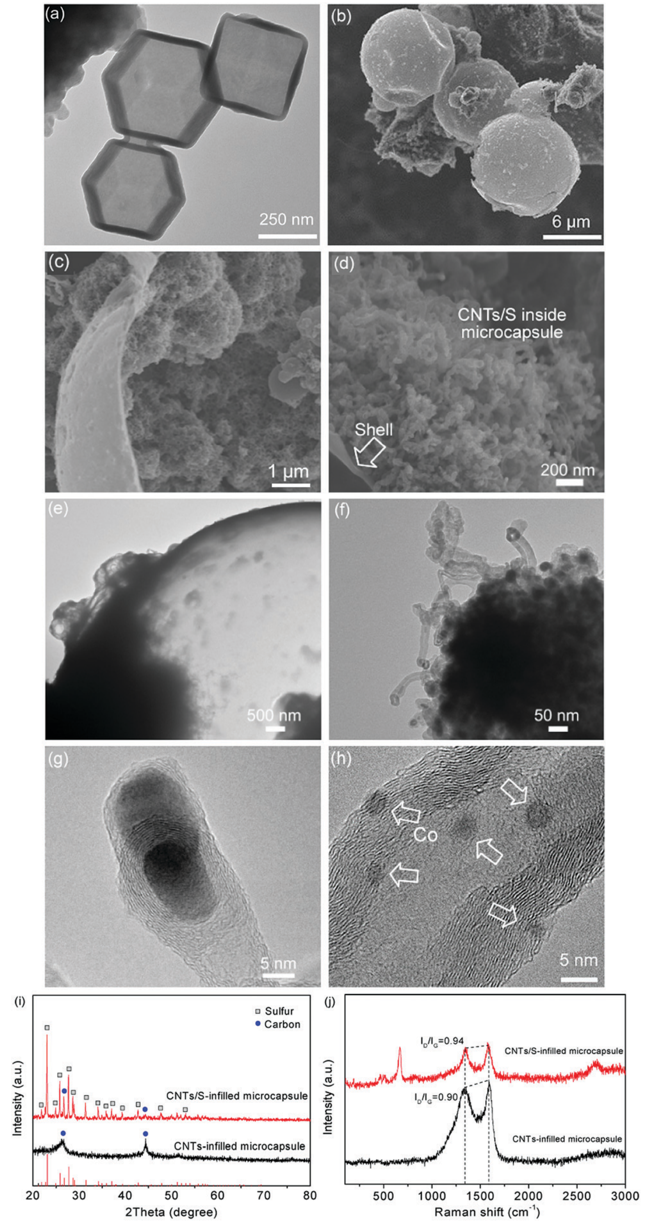

Fig. 2 (a) TEM image of the as-prepared Co_3O_4 nanoboxes. SEM images of the (b) CNT/S-infilled microcapsules and (c, d) a broken microcapsule showing the internal CNTs/S. TEM images of the (e) CNT-grown microcapsule and (f) CNTs. HRTEM images of the (g) tip and (h) inside of a CNT. (i) XRD patterns and (j) Raman spectra of the CNT/S- or CNT-infilled microcapsules.

Results and discussion

The scanning electron microscope (SEM) images of the Co_3O_4 nanoboxes are displayed in Fig. 2a and Fig. S1 (ESI†). The nanoboxes exhibit a morphology of oblate hexagonal prism; on observing the transmission electron microscope (TEM) image, a hollow structure is observed. After encapsulating the nanoboxes and thermal treatment under nitrogen gas, Co_3O_4 was decomposed and reduced, forming some nanoparticles, and leading to the *in situ* catalytical growth of CNTs inside the microcapsules. At last, sulfur was coated into the microcapsules, as shown in Fig. 2b. The microcapsules are about 10 μm in diameter. From a manually-broken microcapsule (Fig. 2c and d), it can be observed that the CNTs/S in the microcapsule are intertwined and connected.

The breaking process was conducted by extruding the microcapsules between two silicon wafers. The CNTs inside the microcapsules and the conductive carbon shell are beneficial to improve the conductivity of the composite; and the microcapsules provide sufficient space, which buffers the structural change of sulfur during charging and discharging.[17] TEM images of the CNT-grown microcapsules (Fig. 2e and f) show the CNT clusters inside. In Fig. 2g, the HRTEM image of the CNT verifies the growth of CNTs induced by Co catalyst.[18] Inside the CNT, there are also some small Co nanoparticles, as shown in Fig. 2h.

The elemental mapping images of the microcapsules in Fig. S2 (ESI†) show that the signal of sulfur on the surface is non-obvious, which is because the additional rapid heat-treatment efficiently removes the external sulfur. By contrast, from the mapping images of a manually-broken microcapsule (Fig. S3, ESI†), the sulfur can be obviously observed and is found located inside the microcapsule. This shows that during sulfur fumigation, sulfur penetrates the microcapsule through the shell. Co is well-dispersed throughout the microcapsule, which is beneficial for the dense growth of CNTs. The energy dispersive spectroscopy (EDS) spectrum (Fig. S3e, ESI†) displays that the microcapsule is composed of C, S, and Co, which are uniformly distributed throughout the microcapsule system. The signal of Si is attributed to the substrate during measurement.

Fig. 2i displays the X-ray diffraction (XRD) patterns of the microcapsules. For the CNT/S-infilled microcapsule, the signal of C shows an expansion around 25°, indicating that it is amorphous in the carbonized microcapsule.[19] The XRD pattern shows the sulfur in the CNT/S-infilled microcapsule, which is in good agreement with the joint committee on powder diffraction standards (JCPDS) card no. 08-0247. Fig. 2j shows the Raman spectra. The peaks at 1351.5 and 1573.2 cm^{-1} in CNT-infilled microcapsules correspond to the D and G bands of carbon, respectively. In addition, it is found that the ratio (I_D/I_G) of microcapsules before sulfur loading is 0.90, while the I_D/I_G of the CNT/S-infilled microcapsule is 0.94, which indicates that the coating of sulfur does not change the carbon structure.[20] Moreover, the peak at about 667 cm^{-1} is ascribed to sulfur.

Thermogravimetric analysis (TGA) of the microcapsules was performed, as shown in Fig. S4a (ESI†). The weight loss between 200 and 300 °C is attributed to sulfur volatilization. The sulfur content of the CNT/S-infilled microcapsules is about 65.5%. The TGA curve shows a loss from 500 °C, corresponding to the decomposition of the carbon shell.[21] The weight retained (10.2%) comes from the CNTs and Co_3O_4 formed by the oxidization of Co. Co has no electrochemical activity in the Li–S battery, so the influence towards the sulfur capacity from Co is neglectable. As shown in Fig. S4b (ESI†), the BET surface area was measured, showing a surface area of 29.1 m^2 g^{-1}. Moreover, pore-size mainly distributes at 1.5 and 5 nm, which indicates that the microcapsule contains both micropores and mesopores. The porosity is beneficial for the uniform distribution of sulfur inside the microcapsules during the loading process, and the ion diffusion.[22,23] Some microcapsules with a relatively higher sulfur content of 74.1% were prepared; and the TGA profile is displayed in Fig. S5 (ESI†). Furthermore, it is confirmed that a sulfur content as high as 91.8% in the microcapsules is achievable (Fig. S6, ESI†), which is significant for improving the overall sulfur loading of the constructed Li–S batteries for potential applications.

In the X-ray photoelectron spectroscopy (XPS) survey spectrum, the elements Co, C, O and S appear (Fig. S7a, ESI†). The Co 2p spectrum shows four peaks (Fig. S7b, ESI†). The peak at 779.9 eV is assigned to Co, while 782.1 eV corresponds to Co $2p_{3/2}$. The one at 782.1 eV is ascribed to Co $2p_{1/2}$.[24] The peaks at 785.7 and 802.6 eV are ascribed to the high-spin Co 2p.[25] In the C 1s spectrum (Fig. S7c, ESI†), C–OH (286.7 eV) and C–C (284.8 eV) are verified.[26] At 164.0 and 165.2 eV, the peaks are attributed to the S–S and S–C bonds, respectively (Fig. S7d, ESI†).[27] The sulfur–oxygen bonding because of the oxidation of sulfur appears at 160 eV, which enhances the interaction between CNTs and sulfur.[28]

Fig. 3a presents the cycling curves of the CNT/S-infilled microcapsules at 0.1C. Here, the sulfur loading of the prepared cathode is about 1.89 mg cm^{-2}. As indicated above, it could be further improved by increasing the sulfur content in the microcapsules. There are two plateaus in the discharge process. The plateau at 2.3 V corresponds to the conversion of sulfur to soluble polysulfides, while the one at 2.05 V is assigned to long-chain sulfides which are further reduced to low-order polysulfides during discharge.[29] Polarization occurs during cycling because of the formation of a solid electrolyte interphase (SEI), which has a poor conductivity. Fig. 3b displays that the initial discharge capacity is 1061 mA h g^{-1}, and after 250 cycles the capacity remains 1010 mA h g^{-1}, which is much higher than that of the CNTs/S prepared by directly coating sulfur onto CNTs that provides a capacity less than 400 mA h g^{-1} and a large capacity decay. The slight increase of the capacity at the initial period could be ascribed to the electrochemical activation caused by the electrolyte diffusion and the porous structure.[30] The coulombic efficiency of the microcapsules remains ≈99.8%, and capacity decay rate is 0.02% per cycle, indicating that the CNT/S-infilled microcapsules possess a good electrochemical stability. This is attributed to the specific microcapsule structure that suppresses the loss of polysulfides. When cycling at 0.3C, the capacity remains 730 mA h g^{-1} after 100 cycles (Fig. S8, ESI†).

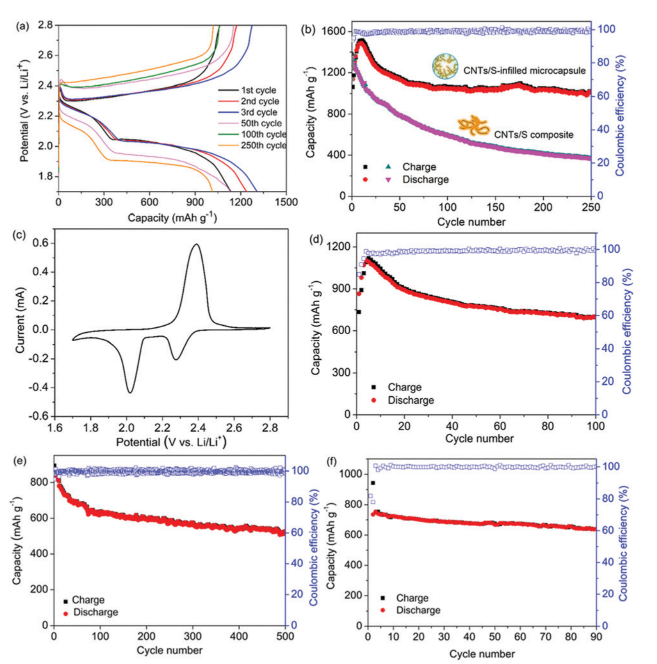

Fig. 3 (a) Charge–discharge curves of the CNT/S-infilled microcapsules at 0.1C. (b) Capacity and coulombic efficiency. (c) CV curve of the CNT/S-infilled microcapsules at 0.1 mA s^{-1}. (d) Electrochemical performance of the microcapsules with a sulfur content of 73.3% at 0.1C. Cycling performance of the microcapsules at (e) 0.3C under −5 °C and (f) 0.1C under 45 °C.

Fig. 3c displays the cyclic voltammetry (CV) curve in which the reduction peaks at 2.02 and 2.27 V are assigned to the conversion of solid S_8 to long-chain polysulfides, and the reduction to short-chain polysulfides. In contrast, the peak at 2.4 V corresponds to the oxidation of polysulfides to S_8.[31] When the sulfur content was increased to 73.3% by using more sulfur powders during the loading process, the capacity exceeds 705 mA h g^{-1} after cycling 100 times (Fig. 3d), indicating a good potential for further increasing the active material loading of the overall Li–S battery. Fig. S9 (ESI†) shows the rate-performance. When cycling at 0.5C, 1C, and 1.5C, the capacities are 1115, 485, and 220 mA h g^{-1}, respectively. Once the rate returns to 0.5C, the battery exhibits a capacity back to 835 mA h g^{-1}. Even after repeating the cycles three times, the capacity keeps 720 mA h g^{-1}. Fig. 3e shows the cycling performance at 0.3C for 500 cycles under a temperature of −5 °C. The initial capacity is 893 mA h g^{-1}, while the capacity remains 523 mA h g^{-1} after cycling 500 times. Fig. 3f displays the performance of the CNT/S-infilled microcapsules under 45 °C at 0.1C. The capacity exceeds 620 mA h g^{-1} after cycling 90 times. For comparison, the CNT/S composite without being encapsulated displays poor capacity and coulombic efficiency (Fig. S10, ESI†).

Fig. 4a presents the electrochemical performance of the CNT/S-infilled microcapsules with different charge *vs.* discharge rates. After cycling 100 times, the capacities remain 580 mA h g^{-1} for 0.4C charging/0.2C discharging, and 521 mA h g^{-1} for 0.2C charging/0.2C discharging (Fig. 4b). The stable performance at different charge *vs* discharge rates also enables the microcapsules to be applicable for constructing Li–S batteries working at different charge/discharge speeds, which is ascribed to the improved conductivity of CNTs for fast transportation of electrons and Li ions. Fig. S11 (ESI†) displays the results of electrochemical impedance spectroscopy (EIS) before and after cycling 250 times at 0.1C. A slight increase of the surface transfer resistance from 95 to 126 Ω can be observed, which further verifies the stable electrochemical properties.

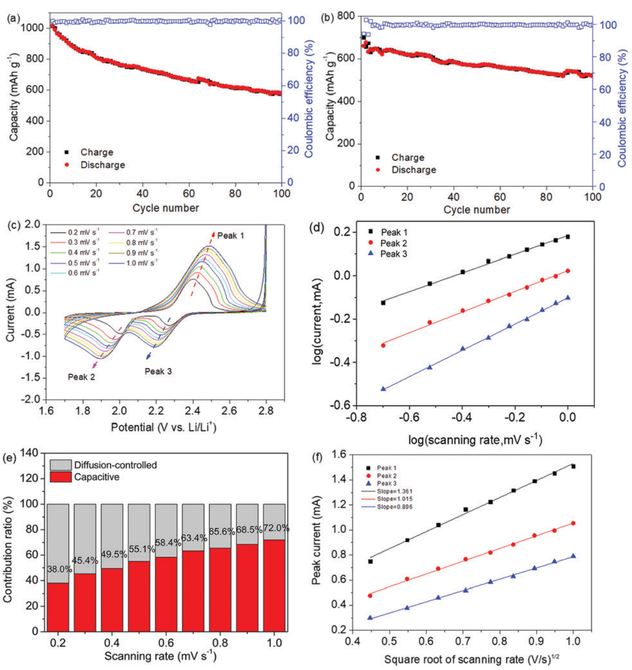

Fig. 4 Cycling performance of the CNT/S-infilled microcapsules under different cycling conditions: (a) charging at 0.4C *vs.* discharging at 0.2C, and (b) charging at 0.2C *vs.* discharging at 0.4C. (c) CV curves at the rates from 0.2 to 1.0 mV s^{-1}. (d) log(i) *vs.* log(ν) plots at peak currents and the fitting results at different redox states. (e) Contribution ratio of the capacitive and diffusion-controlled processes. (f) Plot of CV currents *vs* square root of scanning rates.

The CV curves scanning at 0.2 to 1.0 mV s^{-1} are presented in Fig. 4c. The features of capacitive control and diffusion control of CNT/S-infilled microcapsule are studied according to the following formula: $i = a\nu^b$ and $\log(i) = b\log(\nu) + \log(a)$, where i stands for current density, ν for scan rate and a and b are adjustable parameters. In Fig. 4d, the b values of the anodic and cathodic peaks indicate the diffusion-controlled and capacitive processes, respectively.[32] According to equation $i\,(\mathrm{V}) = k_1\nu + k_2\nu^{1/2}$, the capacitive contribution ($k_1\nu$) and the diffusion-controlled contribution ($k_2\nu^{1/2}$) are obtained.[33] In Fig. 4e, when the rate is higher than 0.4 mV s^{-1}, the capacitive contribution is greater than 50%, which indicates that the sulfur inside the microcapsule is beneficial to the electrochemical reaction with Li ions.[34] Furthermore, the anodic peak current of peak 1 and the cathodic current of peak 2 and peak 3 were linearly fitted to the square root of the scan rate, as shown in Fig. 4f. The capacitive coefficient of Li ions is calculated using the Randles–Sevcik formula. The coefficients for peaks 1 to 3 are 1.583×10^{-9}, 1.181×10^{-9}, and 1.042×10^{-9} cm^2 s^{-1}, respectively, which indicate that the presented all-in-one microcapsule exhibits a good diffusivity compared to those mentioned in some other reports.[35,36]

Conclusion

In summary, we develop a CNT-infilled all-in-one microcapsule as a novel sulfur host prepared by catalytically growing CNTs using reduced Co_3O_4 nanoboxes inside a microcapsule. In the microcapsule, CNTs are beneficial for loading sulfur and improving the conductivity, the microcapsule shell can reduce the loss of polysulfides during cycling, and the void inside the all-in-one microcapsule accommodates the volumetric change of sulfur, enabling good electrochemical stability. A Li–S battery based on the all-in-one microcapsule exhibits a high capacity (1010 mA h g^{-1}) after 250 cycles, a coulombic efficiency of ≈99.8%, and a capacity decay rate of 0.02% per cycle. Furthermore, the battery based in the microcapsules displays stable performance when cycling at both high and low temperatures. It is expected that the presented all-in-one microcapsule system will find broad applications for developing some emerging energy-storage materials and batteries.

Conflicts of interest

There are no conflicts to declare.

Acknowledgements

This work was supported by the Science and Technology Major Project of Anhui Province (18030901093), the Key Research and Development Program of Wuhu (2019YF07), the National Natural Science Foundation of China (11722222), and the Youth Innovation Promotion Association of CAS (2018491).

Notes and references

1 C. Deng, Z. Wang, L. Feng, S. Wang and J. Yu, Electrocatalysis of sulfur and polysulfides in Li–S batteries, *J. Mater. Chem. A*, 2020, **8**, 19704.

2 M. S. Kim, V. Do, Y. Y. Xia, W. Kim and W. I. Cho, Facile and scalable fabrication of high-energy-density sulfur cathodes for pragmatic lithium–sulfur batteries, *J. Power Sources*, 2019, **422**, 104.

3 H. L. Ye, M. Li, T. C. Liu, Y. G. Li and J. Lu, Activating Li_2S as the Lithium-Containing Cathode in Lithium–Sulfur Batteries., *ACS Energy Lett.*, 2020, **5**, 2234.

4 Y. T. Liu, S. Liu, G. R. Li, T. Y. Yan and X. P. Gao, High volumetric energy density sulfur cathode with heavy and catalytic metal oxide host for lithium–sulfur battery, *Adv. Sci.*, 2020, **7**, 1903693.

5 C. Tang, B. Q. Li, Q. Zhang, L. Zhu, H. F. Wang, J. L. Shi and F. Wei, CaO-templated growth of hierarchical porous graphene for high-power lithium–sulfur battery applications, *Adv. Funct. Mater.*, 2016, **26**, 577.

6 Z. Liang, G. Y. Zheng, W. Y. Li, Z. W. Seh, H. B. Yao, K. Yan, D. S. Kong and Y. Cui, Sulfur cathodes with hydrogen reduced titanium dioxide inverse opal structure, *ACS Nano*, 2014, **8**, 5249.

7 Y. Dong and T. Ben, Impregnated sulfur in carbonized nitrogen-containing porous organic frameworks as cathode with high rate performance and long cycle life for lithium–sulfur batteries, *Chem. Res. Chin. Univ.*, 2019, **35**, 654.

8 E. H. M. Salhabi, J. L. Zhao, J. Y. Wang, M. Yang, B. Wang and D. Wang, Hollow multi-shelled structural TiO_{2-x} with multiple spatial confinement for long-life lithium–sulfur batteries, *Angew. Chem., Int. Ed.*, 2019, **58**, 1.

9 J. L. Zhao, M. Yang, N. L. Yang, J. Y. Wang and D. Wang, Hollow micro-/nanostructure reviving lithium–sulfur batteries, *Chem. Res. Chin. Univ.*, 2020, **36**, 313.

10 F. Li, M. R. Kaiser, J. Ma, Y. Hou, T. Zhou, Z. Han, W. Lai, J. Chen, Z. Guo, H. Liu and J. Wang, Uniform polypyrrole layer-coated sulfur/graphene aerogel via the vapor-phase deposition technique as the cathode material for Li–S batteries, *ACS Appl. Mater. Interfaces*, 2020, **12**, 5958.

11 W. W. Sun, C. Liu, Y. J. Li, S. Q. Luo, S. K. Liu, X. B. Hong, K. Xie, Y. M. Liu, X. J. Tan and C. M. Zheng, Rational construction of Fe_2N@C yolk–shell nanoboxes as multifunctional hosts for ultralong lithium–sulfur batteries, *ACS Nano*, 2019, **13**, 12137.

12 W. W. Sun, Y. J. Li, S. K. Liu, Q. P. Guo, Y. H. Zhu, X. B. Hong, C. M. Zheng and K. Xie, Catalytic Co_9S_8 decorated carbon nanoboxes as efficient cathode host for long-life lithium–sulfur batteries, *Nano Res.*, 2020, **13**, 2143.

13 S. Q. Luo, W. W. Sun, J. H. Ke, Y. Q. Wang, S. K. Liu, X. B. Hong, Y. J. Li, Y. F. Chen, W. Xie and C. M. Zheng, A 3D conductive network of porous carbon nanoparticles interconnected with carbon nanotubes as the sulfur host for long cycle life lithium–sulfur batteries, *Nanoscale*, 2018, **10**, 22601.

14 L. Zhou, H. Li, X. C. Wu, Y. Zhang, D. L. Danilov, R. A. Eichel and P. H. L. Notten, Double-shelled Co_3O_4/C nanocages enabling polysulfides adsorption for high-performance lithium–sulfur batteries, *ACS Appl. Energy Mater.*, 2019, **2**, 8153.

15 X. Liao, Z. Li, Q. He, L. Xia, Y. Li, S. Zhu, M. Wang, H. Wang, X. Xu, L. Mai and Y. Zhao, Three-dimensional porous Nitrogen-doped carbon nanosheet with embedded $Ni_xCo_{3-x}S_4$ nanocrystals for advanced lithium–sulfur batteries., *ACS Appl. Mater. Interfaces*, 2020, **12**, 9181.

16 H. Liu, K. Guo, J. Lv, Y. Gao, C. Y. Duan, L. Deng and Z. F. Zhu, A novel nitrite biosensor based on the direct electrochemistry of horseradish peroxidase immobilized on porous Co_3O_4 nanosheets and reduced graphene oxide composite modified electrode, *Sens. Actuators, B*, 2017, **238**, 249.

17 X. Li, X. B. Cheng, M. X. Gao, D. W. Ren, Y. F. Liu, Z. X. Guo, C. X. Shang, L. X. Sun and H. G. Pan, Amylose-derived macrohollow core and microporous shell carbon spheres as sulfur host for superior lithium–sulfur battery cathodes, *ACS Appl. Mater. Interfaces*, 2017, **9**, 10717.

18 G. Mei, L. Cui, Z. Dou and X. He, Heat-treated multi-walled carbon nanotubes-supported (Fe, Co, Ni)-coordinated polyporphyrin: A robust air cathode catalyst for rechargeable zinc-air batteries, *Electrochim. Acta*, 2020, **358**, 136918.

19 R. Qiang, Y. Du, D. Chen, W. Ma, Y. Wang, P. Xu, J. Ma, H. Zhao and X. Han, Electromagnetic functionalized Co/C composites by in situ pyrolysis of metal-organic frameworks (ZIF-67), *J. Alloys Compd.*, 2016, **681**, 384.

20 B. Shao and I. Taniguchi, Synthesis of Li_2MnSiO_4/C nanocomposites for lithium battery cathode employing sucrose as carbon source, *Electrochim. Acta*, 2014, **128**, 156.

21 J. Y. Liu, W. Zhang, Y. Chen, P. Zhou and K. S. Zhang, A novel biomimetic dandelion structure-inspired carbon nanotube coating with sulfur as a lithium–sulfur battery cathode, *Nanotechnology*, 2019, **30**, 155401.

22 R. Zhuang, S. Yao, X. Shen and T. Li, Hydrothermal synthesis of mesoporous MoO_2 nanospheres as sulfur matrix for lithium sulfur battery., *J. Electroanal. Chem.*, 2019, **833**, 441.

23 Z. Cui, J. Yao, T. Mei, S. Zhou, B. Hou, J. Li, J. Li, J. Wang, J. Qian and X. Wang, Strong lithium polysulfides chemical trapping of TiC-TiO_2/S composite for long-cycle lithium–sulfur batteries., *Electrochim. Acta*, 2019, **298**, 43.

24 M. Zhong, J. D. Guan, Q. J. Feng, X. W. Wu, Z. B. Xiao, W. Zhang, S. Tong, N. Zhou and D. X. Gong, Accelerated polysulfide redox kinetics revealed by ternary sandwich-type S@Co/N-doped carbon nanosheet for high-performance lithium–sulfur batteries, *Carbon*, 2018, **128**, 86.

25 P. Wang, Z. Zhang, X. Yan, M. Xu, Y. Chen, J. Li, J. Li, K. Zhang and Y. Lai, Pomegranate-like microclusters organized by

ultrafine Co nanoparticles@nitrogen doped carbon subunits as sulfur hosts for long-life lithium–sulfur batteries, *J. Mater. Chem.*, 2018, **6**, 14178.

26 Y. Zhao, L. Wang, L. Huang, M. Maximov, M. Jin, Y. Zhang, X. Wang and G. Zhou, Biomass-derived oxygen and nitrogen co-doped porous carbon with hierarchical architecture as sulfur hosts for high-performance lithium/sulfur batteries, *Nanomaterials*, 2017, **7**, 402.

27 C. Jin, W. Zhang, Z. Zhuang, J. Wang, H. Huang, Y. Gan, Y. Xia, C. Liang, J. Zhang and X. Tao, Enhanced sulfide chemisorption using boron and oxygen dually doped multi-walled carbon nanotubes for advanced lithium–sulfur batteries, *J. Mater. Chem.*, 2017, **5**, 632.

28 J. S. Lee and A. Manthiram, Hydroxylated N-doped carbon nanotube-sulfur composites as cathodes for high-performance lithium–sulfur batteries, *J. Power Sources*, 2017, **343**, 54.

29 Z. Wang, M. Feng, H. Sun, G. Li, Q. Fu, H. Li, J. Liu, L. Sun, A. Mauger, C. M. Julien, H. Xie and Z. Chen, Constructing metal-free and cost-effective multifunctional separator for high-performance lithium–sulfur batteries, *Nano Energy*, 2019, **59**, 390.

30 Z. B. Xiao, Z. Yang, L. Wang, H. G. Nie, M. E. Zhong, Q. Q. Lai, X. J. Xu, L. J. Zhang and S. M. Huang, A light-weight TiO_2/graphene interlayer, applied as a highly effective polysulfide absorbent for fast, long-life lithium–sulfur batteries., *Adv. Mater.*, 2015, **27**, 2891.

31 J. Wang, J. Polleux, J. Lim and B. Dunn, Pseudocapacitive contributions to electrochemical energy storage in TiO_2 (anatase) nanoparticles, *J. Phys. Chem. C*, 2007, **111**, 14925.

32 X. Huang, Z. L. Wang, R. Knibbe, B. Luo, S. A. Ahad, D. Sun and L. Z. Wang, Cyclic voltammetry in lithium–sulfur batteries-challenges and opportunities, *Energy Technol.*, 2019, **7**, 1801001.

33 W. Tian, H. Hu, Y. Wang, P. Li, J. Liu, J. Liu, X. Wang, X. Xu, Z. Li, Q. Zhao, H. Ning, W. Wu and M. Wu, Metal-organic frameworks mediated synthesis of one-dimensional molybdenum-based/carbon composites for enhanced lithium storage, *ACS Nano*, 2018, **12**, 1990.

34 X. Hu, Y. Li, G. Zeng, J. Jia, H. Zhan and Z. Wen, Three-dimensional networks architecture with hybrids nanocarbon composites supporting few-layer MoS_2 for lithium and sodium storage, *ACS Nano*, 2018, **12**, 1592.

35 Z. J. Liu, B. L. Liu, P. Q. Guo, X. N. Shang, M. Z. Lv, D. Q. Liu and D. Y. He, Enhanced electrochemical kinetics in lithium–sulfur batteries by using carbon nanofibers/manganese dioxide composite as a bifunctional coating on sulfur cathode, *Electrochim. Acta*, 2018, **269**, 180.

36 J. W. Zhang, Q. Q. Rao, B. Y. Jin, J. G. Lu, Q. G. He, Y. Hou, Z. P. Li, X. L. Zhan, F. Q. Chen and Q. H. Zhan, Cerium oxide embedded bilayer separator enabling fast polysulfide conversion for high-performance lithium–sulfur batteries, *Chem. Eng. J.*, 2020, **388**, 124120.

